Molecular Therapy
Methods & Clinical Development
Original Article

Treatment of experimental autoimmune encephalomyelitis using AAV gene therapy by blocking T cell costimulatory pathways

Chen Zhong,[1] Zifeng Chen,[1] Yong Xia,[2] Jun Wu,[1] Feixu Zhang,[1] Cheng Cheng,[2] Xia Wu,[2] Yingping Zhuang,[1] and Xiao Xiao[1,2,3]

[1]State Key Laboratory of Bioreactor Engineering, School of Biotechnology, East China University of Science and Technology, Shanghai 200237, China; [2]School of Pharmacy, East China University of Science and Technology, Shanghai 200237, China; [3]Division of Pharmacoengineering and Molecular Pharmaceutics, Eshelman School of Pharmacy, University of North Carolina, Chapel Hill, NC 27517, USA

Multiple sclerosis (MS) is a chronic autoimmune disease of the central nervous system (CNS), characterized by inflammation and demyelination. Presently, repeated relapses of MS necessitate long-term immune-regulatory therapy. Blocking the CD28-B7 and CD40-CD40L costimulatory pathways is an effective and synergistic method for the prevention and amelioration of clinical symptoms of experimental autoimmune encephalomyelitis (EAE), a mouse model of MS. In this study, to explore the efficacy and safety of MS gene therapy, we used adeno-associated virus (AAV) as a vector to deliver CTLA4-immunoglobulin (Ig) or CD40-Ig on the EAE induced by myelin oligodendrocyte glycoprotein (MOG). Our results showed that a single administration of AAV8-CTLA4-Ig, either alone or with AAV8-CD40-Ig, protected mice from EAE and reversed disease progression. Decreased $CD4^+$ and $CD8^+$ T cell infiltration, inhibition of MOG antibody response, and downregulation of neuroinflammation were observed in mice receiving AAV, suggesting that autoimmunity was suppressed in EAE pathology. Moreover, no hematological or hepatic toxicity was observed in AAV-treated mice. Thus, compared with treatment with recombinant CTLA4-Ig (belatacept), AAV gene therapy could effectively control clinical symptoms and suppress autoimmunity in the long term. In summary, our study provides a potential therapeutic method for blocking T cell costimulation for the treatment of MS via gene therapy.

INTRODUCTION

Multiple sclerosis (MS) is an autoimmune disease characterized by inflammatory demyelination in the central nervous system (CNS), with complicated pathogenesis related to genetic genes and certain environmental factors, such as the Epstein-Barr virus (EBV), UV light, and vitamin D.[1,2] There are currently more than 2.3 million people worldwide with MS.[3] Presently, typical treatment for MS involves disease-modifying therapies (DMTs), which aim to treat symptoms and manage relapses.[1] However, most DMTs to treat MS have been unsuccessful, due to toxicity or failure to inhibit pathology in the long term.[4,5] A humanized anti-CD25 monoclonal antibody (mAb) has been approved by the Food and Drug Administration for a reduction in annual relapse rates in relapsing remitting MS (RRMS) but poses the risk of liver toxicity.[6–8] Immunomodulators, such as interferon-β 1a and 1b, alleviate relapses of secondary progressive MS (SPMS) but have failed in controlling permanent disability.[9–11] Consequently, a long-term, effective, and safe strategy against MS in clinics is required.

Autoreactive $CD4^+$ T cells, mainly T helper (Th) 1 and Th-17 cells, are thought to initiate and mediate MS progression.[12,13] Interleukin-17 (IL-17), from Th-17 cells,[14] whose secretion is possibly associated with IL-23,[15] is reported to have enhanced expression in MS disease activity and active lesions.[16,17] $CD4^+$ and $CD8^+$ T cells exist in different lesion regions,[18,19] and $CD8^+$ T cells play a critical role in MS development. Moreover, although MS is a T-cell-mediated disorder, the therapeutic efficacy of anti-CD20 mAb demonstrates the importance of B cells in pathogenesis.[20,21] In acute lesions of the CNS, B cells could potentially be involved in autoantibody production, antigen presentation to T cells, and cytokine secretion to regulate T cells.[22]

Several studies have confirmed that CTLA4-immunoglobulin (Ig), anti-CD40, or CD40L mAbs are effective in the treatment of certain autoimmune diseases in animal models, such as MS[23–25] and lupus nephritis.[26,27] Notably, Schaub et al.[28] found that CTLA4-Ig combined with MR1 (an anti-CD40L mAb) had a synergistic effect in ameliorating ongoing experimental autoimmune encephalomyelitis (EAE), suggesting that the concomitant blocking of the CD28-B7 and CD40-CD40L pathways is more effective in RRMS. Despite the

Received 7 December 2021; accepted 25 April 2022;
https://doi.org/10.1016/j.omtm.2022.04.011.

Correspondence: Xia Wu, PhD, School of Pharmacy, East China University of Science and Technology, Shanghai 200237, China.
E-mail: wuxia@ecust.edu.cn
Correspondence: Xiao Xiao, PhD, State Key Laboratory of Bioreactor Engineering, School of Biotechnology, East China University of Science and Technology, Shanghai 200237, China.
E-mail: xxiao@email.unc.edu

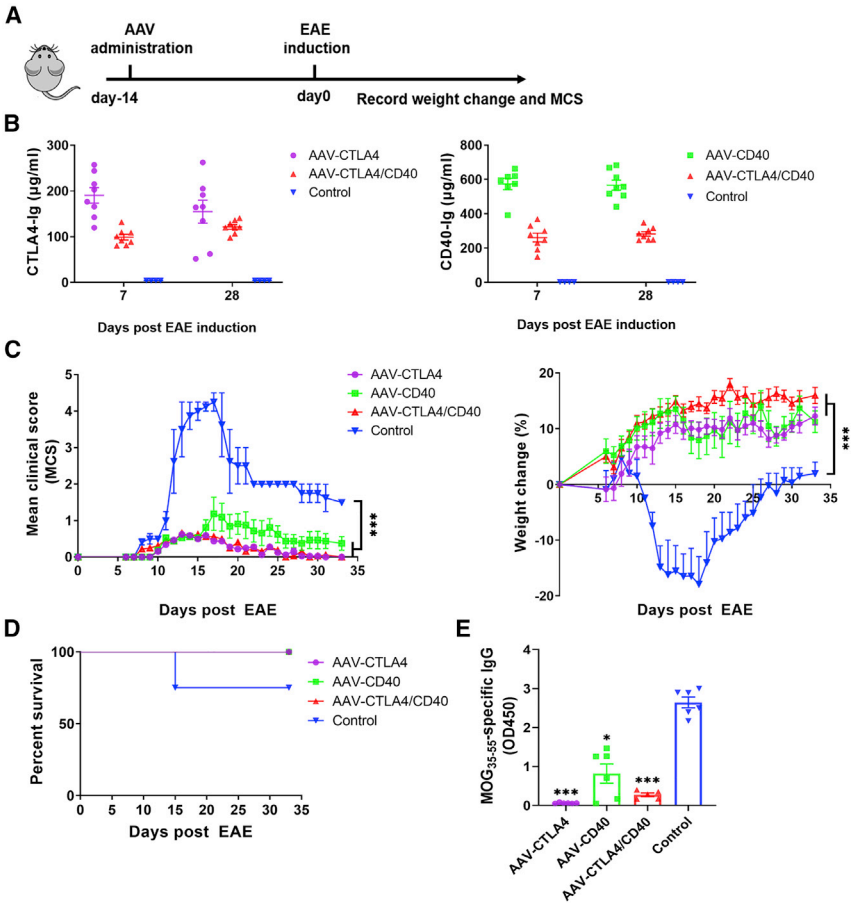

Figure 1. AAV-delivered CTLA4-Ig or CD40-Ig protects mice from clinical symptoms of EAE disease

(A) Study design for *in vivo* prophylactic experiment (n = 8–10 per group). EAE mice without AAV injection were controls. (B) CTLA4-Ig and CD40-Ig levels in mice serum were determined by ELISA. (C) Mean clinical score (MCS) and weight were recorded daily from day 7 post-EAE induction. Percentage of weight change was related to weight at day 0. Two-way ANOVA followed by Tukey posttest is shown. (D) Mice survival was determined until day 35. (E) MOG_{35-55} specific IgG levels in mice serum were determined by ELISA. One-way ANOVA followed by Dunnett posttest is shown. Each value represents the mean ± SEM. *p < 0.05 and ***p < 0.001, compared with control. OD450, optical density 450.

therapeutic advantages of CTLA4-Ig in the murine MS model, the drug was not effective in reducing disease activity in a phase-II, placebo-controlled study of abatacept (CTLA4-Ig) in RRMS,[29] and the exact reason for this remains unclear.[30]

Considering the life-long disease progression of MS, long-term immune modulating therapies are necessary. Gene therapy is a convenient and effective strategy to deliver therapeutic genes and achieve stable and long-term expression. Adeno-associated viruses (AAVs) have been widely applied in gene therapy due to their low immunogenicity and long-lasting transgene expression.[31,32] Several studies have used AAV gene therapy for treating MS and other autoimmune disorders in mice models.[33–37] In this study, we investigate the efficacy of AAV8-CTLA4-Ig or AAV8-CD40-Ig alone or with a combination of AAV8-CTLA4-Ig and AAV8-CD40-Ig in the prevention and reversal of EAE in mice. The results showed that AAV8-CTLA4-Ig either alone or with AAV8-CD40-Ig effectively protected mice from developing severe EAE and reversed clinical symptoms. In addition, compared with recombinant CTLA4-Ig (belatacept), AAV gene therapy inhibited immune cells activation and myelin oligodendrocyte glycoprotein (MOG) antibody production, as well as controlled disease development of EAE in the long term.

RESULTS

AAV-delivered CTLA4-Ig or CD40-Ig protected from clinical symptoms of EAE

In order to investigate whether CTLA4-Ig or CD40-Ig delivered by AAV could prevent EAE, mice were injected intravenously with 2×10^{12} vector genome (vg)/kg of AAV8-CTLA4-Ig or AAV8-CD40-Ig or a mixture of 2×10^{12} vg/kg each of AAV8-CTLA4-Ig and AAV8-CD40-Ig 14 days prior to EAE induction (Figure 1A). Henceforth, AAV8-CTLA4-Ig, AAV8-CD40-Ig, and AAV8-CTLA4-Ig combined with AAV8-CD40-Ig are abbreviated as AAV-CTLA4, AAV-CD40, and AAV-CTLA4/CD40, respectively. At day 28, transgene CTLA4-Ig and CD40-Ig were stably expressed above 100 and 300 μg/mL, respectively (Figure 1B). Mean clinical score (MCS) results showed that mice treated with AAV had mild or even no symptoms, compared with control mice (***p < 0.001; Figure 1C). The MCS of the AAV-CD40 group was higher than that of the AAV-CTLA4-engaged group, including during the peak and later stages of disease progression. Mice without treatment displayed significant weight loss after onset (***p < 0.001; Figure 1C) and 25% of them died (Figure 1D). MOG_{35-55} immunoglobulin G (IgG), an IgG related to EAE disease development,[35] was evidently inhibited in AAV-treated mice compared with control, and AAV-CTLA4-engaged groups produced a weaker MOG antibody response (Figure 1E). These results show that gene therapy with AAV can protect mice from developing severe EAE disease.

AAV gene therapy suppressed immune cells activation and inflammatory cytokines production

To investigate the prophylactic effect of AAV administration on innate immune cells and inflammatory cytokines in the CNS, we assayed a number of astroglia and microglia, as well as the cytokines tumor necrosis factor alpha (TNF-α), interferon (IFN)-γ, IL-1β, IL-6, IL-17, and IL-23 of the spinal cord. Activated astroglia and microglia are important drivers of progressive MS.[38] Based on integrated

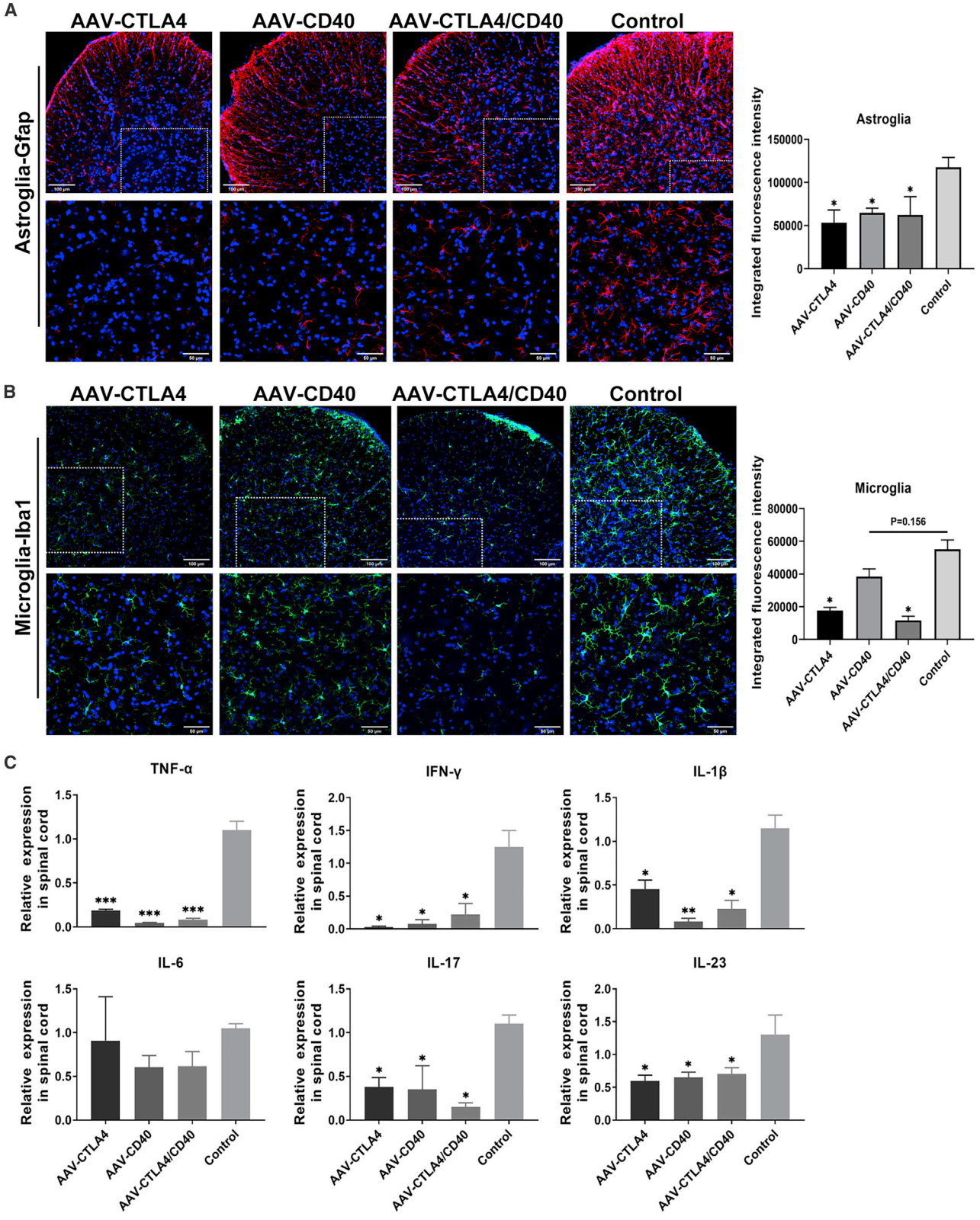

(legend on next page)

fluorescence intensity, although the other AAV-administered groups showed fewer astroglia and microglia than the control group (*$p < 0.05$; Figures 2A and 2B), the AAV-CD40 group showed no significant difference in microglia numbers ($p = 0.156$). Th-1 cell cytokines, TNF-α, IFN-γ, IL-1β, IL-17, and IL-23, were significantly downregulated in mice treated with medicative AAV, whereas IL-6, from Th-2 cells, was only slightly reduced in treated mice (Figure 2C). These results show that the prophylactic administration of AAV strongly inhibits astroglial and microglial activation and reduces inflammatory cytokines in the spinal cord.

AAV gene therapy protected from pathologic signs of EAE

MS is characterized by encephalitogenic inflammation, demyelination, and $CD4^+$ and $CD8^+$ T cell infiltration.[39] Hematoxylin and eosin (H&E) staining, Luxol Fast Blue (LFB) staining, and CD4 and CD8 immunohistochemistry of the lumbar spinal cord were conducted in mice to determine their neurological deficits. Histological analysis showed that AAV-treated mice had little to no inflammatory foci, demyelination of white matter (Figures 3A and 3B), or $CD4^+$ T and $CD8^+$ T cell infiltration (Figures 3C and 3D). In contrast, control mice possessed severe pathological features, particularly demyelination and $CD4^+$ T cell infiltration. These results suggest that gene therapy with AAV protects mice from inflammation and myelin loss.

AAV-delivered CTLA4-Ig or CD40-Ig reversed end-stage EAE

Next, we investigated whether AAV immunosuppression treatment could reverse established and even advanced EAE. Mice received 5×10^{12} vg/kg of AAV-CTLA4 or AAV-CD40 or a mixture of 5×10^{12} vg/kg each of AAV-CTLA4 and AAV-CD40 when their MCS reached 2.0, indicating end-stage EAE (Figure 4A). All mice began to develop EAE from day 7–9 and reached a peak at day 18. The peak MCS was 4.04 ± 0.78 for the control group, 2.07 ± 0.53 for the AAV-CTLA4, 2.91 ± 0.64 for the AAV-CD40 group, and 2.57 ± 1.28 for the AAV-CTLA4/CD40 group (Figure 4B). After remission, the mice underwent a short relapse and reached a plateau by day 34. By then, the clinical scores were significantly reduced. On day 59, these were 0.79 ± 0.53, 1.30 ± 0.32, and 1.14 ± 0.19 for the AAV-CTLA4, AAV-CD40, and AAV-CTLA4/CD40 group, respectively, while the control group had a clinical score of 3.01 ± 0.4. The mice in the AAV-CTLA4 group gained the most weight after remission, while mice in the AAV-CD40 and AAV-CTLA4/CD40 groups gained weight after day 34 (Figure 4B). The survival of mice in AAV-CTLA4, AAV-CD40, and AAV-CTLA4/CD40 groups was significantly improved compared with that of the control group (87.5%, 87.5%, and 100%, respectively, versus 75%) (Figure 4C). Lower levels of $MOG_{35–55}$ IgG were observed in AAV-treated mice: AAV-CTLA4-engaged groups produced weak MOG antibody responses, and only the AAV-CTLA4/CD40 group showed a significant difference compared with the control group ($p = 0.0001$; Figure 4D). These results show that gene therapy with AAV has the potential to reverse the clinical symptoms of end-stage EAE.

AAV gene therapy inhibited inflammatory cytokines production and reversed signs of pathology

We assayed TNF-α, IFN-γ, IL-1β, IL-6, IL-17, and IL-23 levels in the spinal cord and spleen. The results showed that IFN-γ and IL-17 in the spinal cord and spleen were strongly inhibited in mice receiving AAV compared with the control (Figures 5A and 5B). Low levels of TNF-α and IL-1β were detected in AAV-treated mice, although there were no significant differences compared with control (Figure 5A). AAV-CTLA4-engaged groups had significantly lower splenic IL-17 and IL-23 (Figure 5B). In addition, splenic IL-6 was strongly reduced in AAV administration groups (Figure 5B).

At day 60, spinal cords of the mice were collected and lumbar regions were stained with LFB. Severe demyelination within the white matter was observed in control mice. Conversely, barely any myelin damage was observed in AAV-treated mice (Figure 5C). The results indicate that gene therapy with AAV effectively inhibits inflammatory cytokine production and reverses pathological lesions in end-stage EAE.

AAV gene therapy had better efficacy on developing EAE than recombinant CTLA4-Ig

To compare the therapeutic effects of AAV gene therapy and recombinant CTLA4-Ig protein (belatacept), mice were injected intravenously with 5×10^{12} vg/kg of AAV-CTLA4 or AAV-CD40 or a mixture of 5×10^{12} vg/kg each of AAV-CTLA4 and AAV-CD40 4 days after EAE induction (early-stage EAE). Concurrently, in the belatacept group, mice were injected intraperitoneally with 100 μg belatacept on alternate days for seven doses (Figure 6A). The MCS of mice receiving AAV or belatacept was lower than that of control mice (Figure 6B). Belatacept-treated mice had slight clinical symptoms before day 16 but gradually developed EAE, and the final MCS on day 43 was 1.31 ± 1.19. The AAV-CTLA4 and AAV-CTLA4/CD40 groups had no clinical symptoms except the limp tail tip, and the final MCS was 0.13 ± 0.12 and 0, respectively. The MCS of mice in the AAV-CD40 group peaked at day 14, and final MCS was 0.83 ± 0.14. Mice in the belatacept group lost weight after day 17, those in the AAV-CD40 group lost weight during days 12–17, while the AAV-CTLA4-enaged mice showed continued weight gain (Figure 6B). Strikingly, three belatacept-treated mice died after day 12, whereas the AAV-treated mice survived (Figure 6C). Mice with AAV therapy had a weaker MOG antibody response; however, there was a comparable level of $MOG_{35–55}$ IgG in mice treated with belatacept compared with the control (Figure 6D). These findings suggest that AAV gene therapy has better efficacy in controlling

Figure 2. Characterization of the prophylactic effect of AAV therapy on innate immune cells and inflammatory cytokines

Amounts of astroglia (A) and microglia (B) in spinal cord were assayed with specific markers glial fibrillary acidic protein (Gfap) and ionized calcium binding adapter molecule 1 (Iba1) by immunofluorescence, respectively (n = 5 per group). Representative images of integrated fluorescence intensity were quantified. The scale bar in the upper row represents 100 μm and in the lower row 50 μm. (C) Inflammatory cytokines TNF-α, IFN-γ, IL-1β, IL-6, IL-17, and IL-23 of the spinal cord were tested via qRT-PCR (n = 4–5 per group). Each value represents the mean ± SEM. *$p < 0.05$, **$p < 0.01$, and ***$p < 0.001$, compared with control. One-way ANOVA followed by Dunnett posttest is shown.

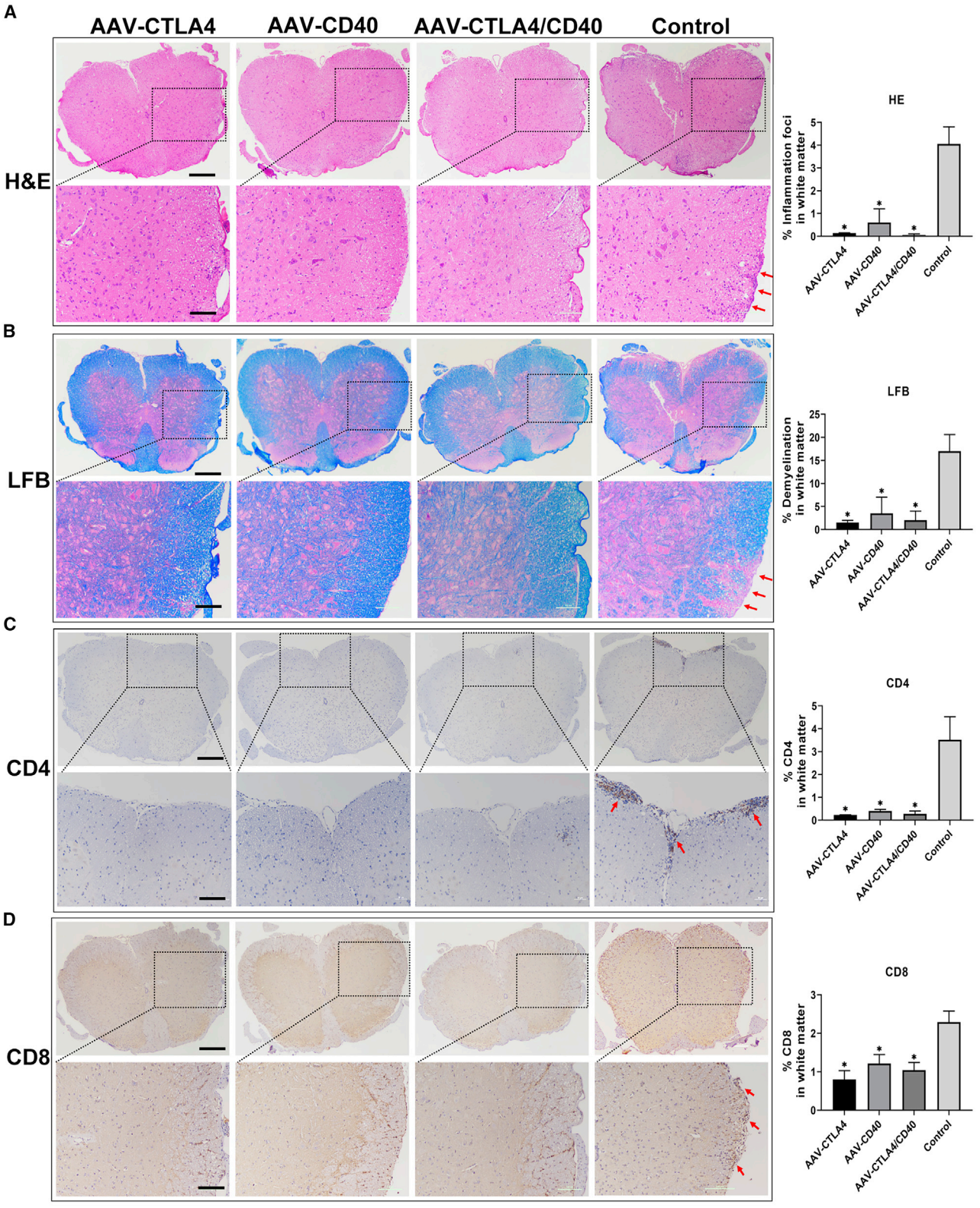

(legend on next page)

clinical symptoms and inhibiting the MOG immune response than recombinant CTLA4-Ig.

AAV gene therapy had better immunosuppression on immune cells than recombinant CTLA4-Ig

To compare the effects of AAV gene therapy and belatacept therapy on innate and adaptive immune cells, the number of astroglia, microglia, $CD4^+$ T, $CD8^+$ T, and $B220^+CD19^+$ B cells of spinal cord were assayed. We found that the total number of lymphocytes in all groups was not significantly different, suggesting that AAV or belatacept administration selectively inhibits immune cells (Figure 7A). $CD4^+$ T and $CD8^+$ T cells were significantly reduced in mice treated with AAV (Figures 7B and 7C). Belatacept-treated mice also had reduced levels of $CD4^+$ T and $CD8^+$ T cells, though the difference was not statistically significant. Interestingly, mice receiving AAV therapy had low $B220^+CD19^+$ B cells compared with control, but no significant differences were detected in levels of $B220^+CD19^+$ B cells in all groups (Figure 7D). Astroglia were significantly inhibited in AAV-CTLA4-engaged groups; their levels were reduced in the belatacept group (Figure 7E). Microglia were noticeably suppressed in AAV gene therapy (excluding AAV-CD40) groups and the belatacept therapy group (Figure 7F). These results demonstrate that AAV immunotherapy had better efficacy in inhibiting innate and adaptive cells in early-stage EAE.

Sustained expression of immune inhibitory protein mediated by AAV had no hematological and hepatic toxicity

To investigate the safety of long-term expression of transgenes delivered by AAV, plasma alanine aminotransferase (ALT) and aspartate aminotransferase (AST) levels were tested. ALT and AST were measured as indicators of liver injury.[35] In prophylactic experiments, at 7 days post-injection, the mice receiving AAV-CTLA4 and AAV-CD40 experienced a significant increase in ALT and AST, respectively (Figure 8A). However, at 35 days post-injection, transaminase levels settled down, with no significant differences compared with healthy control. In therapeutic experiments, the ALT and AST activity detected in all groups at the end of study was within the normal range of mice (Figures 8B and 8C). To further analyze hepatotoxicity of AAV therapy, on day 60, liver tissues were stained with H&E. Histological analysis showed no evident inflammation infiltration in mice receiving AAV (Figure 8D). Peripheral blood cells, including white blood cells, lymphocytes, granulocytes, red blood cells, hemoglobin, and platelets, were assayed, without significant differences among all groups, which suggested no hematologic toxicity of AAV administration (Figure 8E).

DISCUSSION

MS is a heterogeneous autoimmune disease for which no effective cure currently exists.[36] Numerous drugs aimed at the complex mechanisms of MS progression are being explored. These mechanisms include immune system, neuronal dysfunction and metabolic disturbances caused by mitochondrial lesions. Previously, blocking the CD28-B7 or CD40-CD40L pathway was considered an effective way of controlling murine EAE.[40–45] Considering the chronic disease characteristics of MS, effective disease treatment requires continuous immunotherapy. Therapeutic genes delivered by AAV may be an effective form of treatment, since these can sustain stable and persistent expression *in vivo*.[46]

In this study, we investigated the efficacy of a single administration of the AAV8 vector carrying CTLA4-Ig or CD40-Ig in the prevention and reversal of EAE induced by MOG, an animal model of MS. The results showed that AAV8-CTLA4-Ig or AAV8-CD40-Ig alone, or in combination, could protect mice from developing severe EAE and reverse clinical symptoms at various stages of EAE. It was observed that the administration of AAV8-CD40-Ig was not as effective as AAV8-CTLA4-Ig in the reversal of EAE symptoms (Figures 4B and 6B), possibly due to the inferior immunosuppression of CD40-Ig. This was also demonstrated in our previous study of immunocompetent mice, in which AAV vectors expressing CTLA4-Ig or CD40-Ig were used to achieve repeated systemic doses of AAV.[47]

It has been reported that CD28-B7 and CD40–CD40L costimulatory pathways, when blocked, have a synergistic effect on the prevention and reversal of EAE pathology.[28] Interestingly, we found that the combination of AAV8-CTLA4-Ig and AAV8-CD40-Ig was slightly inferior to AAV8-CTLA4-Ig in controlling clinical symptoms of end-stage EAE (Figure 4B). This could be because blocking CD40–CD40L interaction inhibits early disease progression in EAE[45,48] and the CD40–CD40L pathway is thought to provide signal transduction for B cell activation.[49] Certain B cells have a dual role in the pathogenesis of MS: they induce autoimmunity and reconcile inflammatory infiltration of the CNS.[50–52] The combination treatment may have performed not much better because B cells possibly regulate inflammation in the end-stage EAE. It is worth noting that mice receiving combination AAV had significantly lower $MOG_{35–55}$ IgG in end-stage EAE (Figure 4D), and in EAE, MOG is considered a target of the antibody-mediated immune response.[53] There was an enhanced anti-MOG antibody level in the cerebrospinal fluid of MS patients.[54] We found that anti-MOG antibodies did not completely correlate with clinical symptoms, suggesting that these antibodies did not directly participate in disease progression of EAE, which is consistent with existing literature.[55]

In EAE, spinal cord is the initiate region of encephalitogenic impairment, such as inflammation and demyelination.[56] Histological

Figure 3. Persistent expression of CTLA4-Ig or CD40-Ig protects mice from pathological signs

Histological analysis of lumbar spinal cord was conducted (n = 5 per group). H&E staining of inflammation infiltration of white matter (A), Luxol Fast Blue (LFB) staining of demyelination (B), and CD4 (C) and CD8 (D) immunohistochemistry were exhibited. The scale bar in the upper row represents 500 μm and in the lower row 100 μm. Red arrows indicate pathological regions. The respective statistical analysis was in the right panel. The bar graphs show the percentage of inflammation, demyelination, or CD4- or CD8-positive areas in the total white matter. Each value represents the mean ± SEM. *$p < 0.05$, compared with control. One-way ANOVA followed by Dunnett posttest is shown.

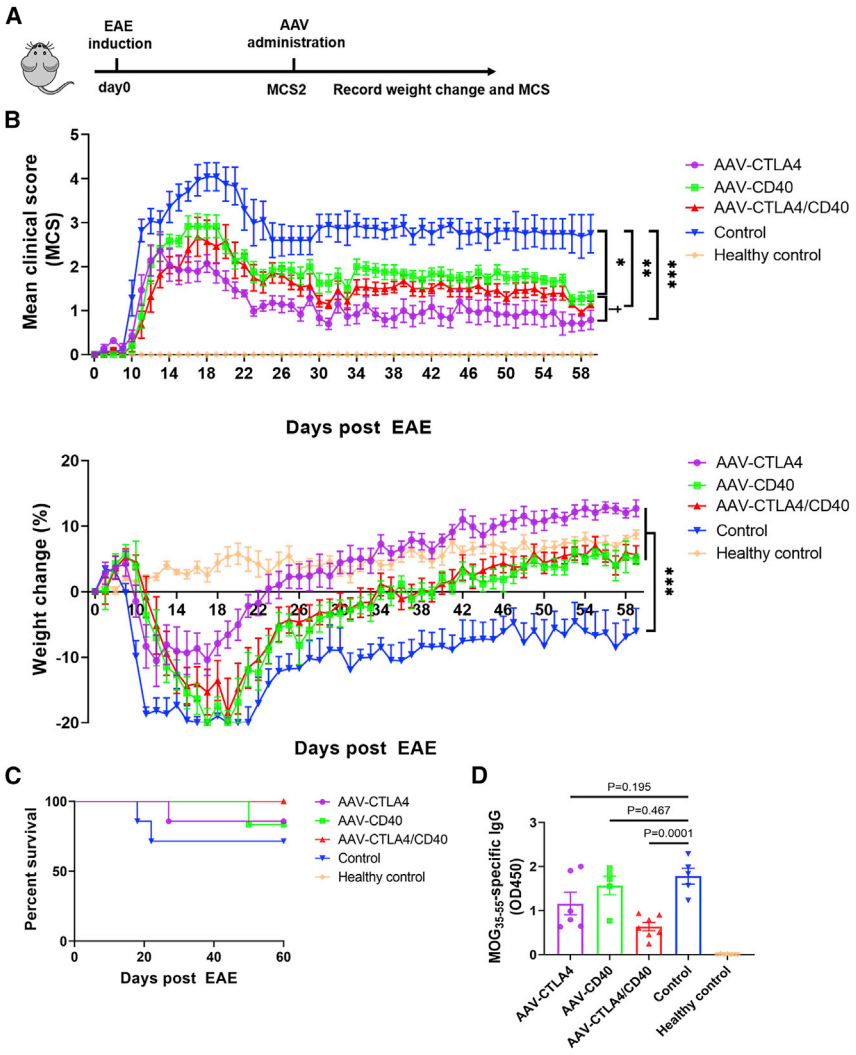

Figure 4. AAV-delivered CTLA4-Ig or CD40-Ig reversed end-stage EAE

(A) Study design for *in vivo* therapeutic experiments (n = 8–10 per group). EAE mice without AAV injection were controls; untreated wild-type mice were healthy controls. (B) MCS and weight were recorded daily from day 7 post-EAE induction. Two-way ANOVA followed by Tukey posttest is shown. †$p < 0.05$, AAV-CTLA4 compared with AAV-CD40. (C) Mice survival was determined until day 60. (D) MOG_{35-55} specific IgG levels in mice serum were determined by ELISA. One-way ANOVA followed by Dunnett posttest is shown. *$p < 0.05$, **$p < 0.01$, and ***$p < 0.001$, compared with control. Each value represents the mean ± SEM.

analysis of the spinal cord of mice showed that mice receiving AAV barely had inflammatory foci and demyelination of white matter, even at end-stage EAE (Figure 5C). Innate immune cells, including astrocytes and microglia, were significantly downregulated in the AAV8-CTLA4-Ig-engaged groups. Astrocytes recruit inflammatory monocytes to the CNS and produce neurotoxic molecules, such as TNF-α, aggravating disease progression.[57,58] TNF-α, IFN-γ, IL-1, and IL-6 are related to activated microglia and damage oligodendrocytes.[59] In our study, pro-inflammatory cytokines TNF-α, IFN-γ, IL-1β, IL-17, and IL-23 from the spinal cord and spleen were inhibited in mice treated with AAV.

In order to explore the clinical translational value of AAV therapy on MS, we compared the therapeutic efficacy of gene therapy with recombinant CTLA4-Ig. In one study, in phase-II clinical trials, for reasons unknown, recombinant CTLA4-Ig had exhibited no clinical benefits. From MCS results, it could be seen that, although initially belatacept delayed EAE onset and controlled disease progression, afterward, its diminished effects led to EAE development. The increasing tendency of MCS after day 15 suggested that belatacept treatment had strongly ameliorated clinical EAE in the preceding time (Figure 6B). This finding is consistent with the strong inhibition of microglia observed in belatacept-treated mice (Figure 7F). Microglia become activated early in EAE and then differentiate into macrophage-like and dendrite-like cells in the CNS, whose function possibly involves antigen presentation to encephalitogenic T cells.[38] This also suggests that the reduction of microglia infiltrates seems to only partially correlate with the rescue of the clinical score. It was possible that a short half-life and un-sustained plasma concentration led to the invalidation of belatacept. The pharmacokinetic parameters of mice treated with a single typical dose of 0.29 mg of CTLA4-Ig intravenously show C_{max} of 290 μg/mL and half-life ($t_{1/2}$) of 59.2 h.[60] In our study, CTLA4-Ig and CD40-Ig expression mediated by AAV8 was stable and sustained, and CTLA4-Ig maintained concentrations above 100 μg/mL 42 days post-AAV injection (Figure 1B). We suggest that it was the persistent expression of immune inhibitory proteins delivered by AAV that achieved a long-term control of EAE pathology. It is also possible that continuous injection of belatacept could achieve similar effect. Moreover, no hematological and hepatic toxicity was observed in AAV immunotherapy.

In conclusion, AAV8-CTLA4-Ig, either alone or with AAV8-CD40-Ig, is effective in protecting from severe EAE and reversing clinical symptoms in the long term. Thus, gene therapy treatment using AAV8-CTLA4-Ig is superior to commercially available recombinant CTLA4-Ig therapy. Nonetheless, the failure of abatacept (CTLA4-Ig) treatments in a clinical trial of RRMS vividly reminds us the limitation of this strategy. Additional in-depth research and alternative approaches are required before any consideration of clinical translation of AAV gene therapy for MS, for example, regulated and inducible therapeutic gene expression and combination with other therapeutic

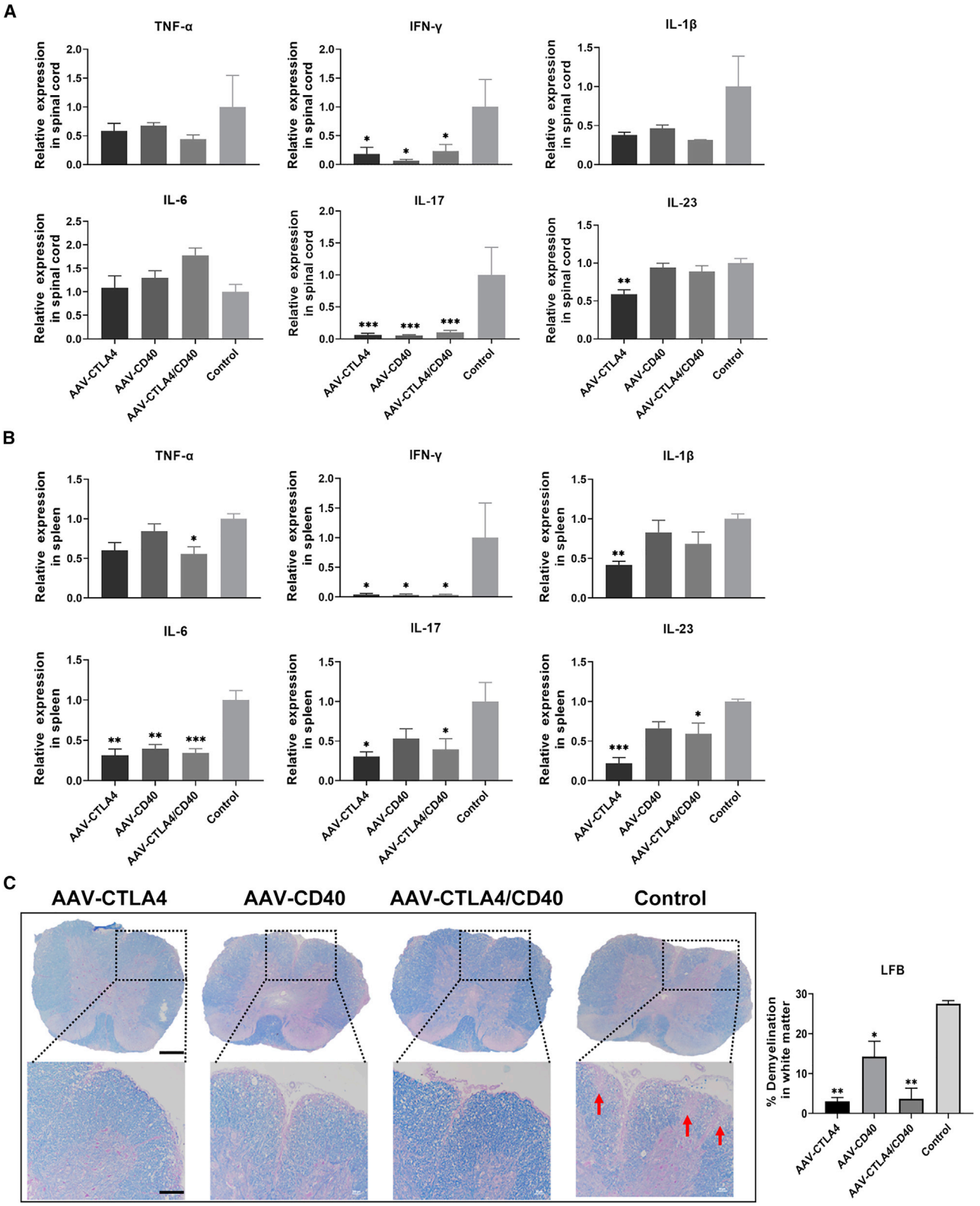

(legend on next page)

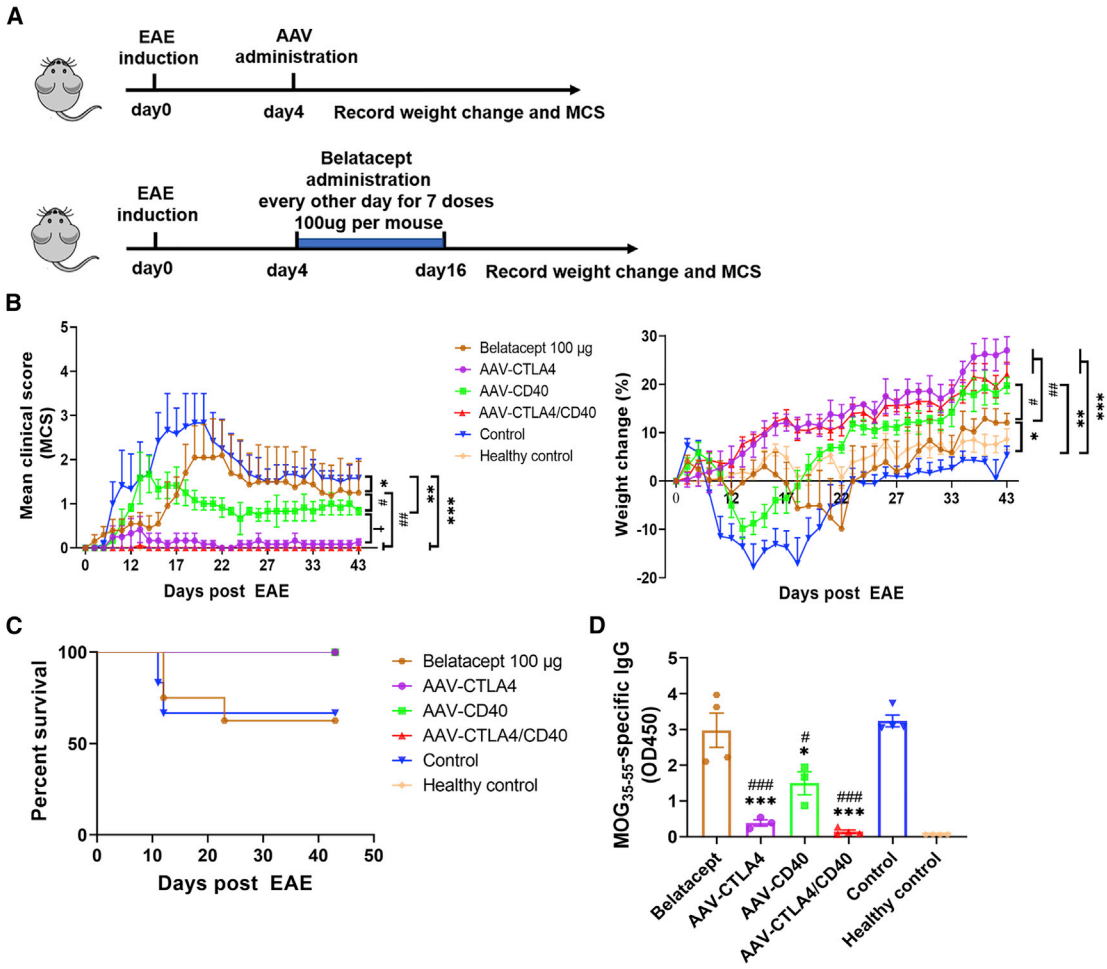

Figure 6. Comparing therapeutic effect of gene therapy and recombinant CTLA4-Ig on developing EAE

(A) Study design outline for *in vivo* therapeutic experiments (n = 8–10 per group). EAE mice without administration were controls; untreated wild-type mice were healthy controls. (B) MCS and weight were recorded daily from day 7 post-EAE induction. Two-way ANOVA followed by Tukey posttest is shown. $^{\dagger}p < 0.05$, AAV-CTLA4 compared with AAV-CD40. (C) Mice survival was determined until day 45. (D) MOG_{35-55} specific IgG levels in mice serum were determined by ELISA. One-way ANOVA followed by Tukey posttest is shown. $^{*}p < 0.05$, $^{**}p < 0.01$, and $^{***}p < 0.001$, compared with control; $^{\#}p < 0.05$, $^{\#\#}p < 0.01$, and $^{\#\#\#}p < 0.001$, compared with belatacept. Each value represents the mean ± SEM.

modalities. Thorough safety evaluations need to be conducted in preclinical studies and clinical trials.

MATERIALS AND METHODS

AAV vector construction

The transgene plasmids pAAV-CTLA4-Ig and pAAV-CD40-Ig (abbreviated as pAAV-CTLA4 and pAAV-CD40) contained extracellular domains of human CTLA4 and CD40 ligated to the Fc portion of the human IgG heavy chain (defined as CTLA4-Ig or CD40-Ig), respectively. The AAV8 vector genome contained AAV2 terminal repeats, a CB promoter (CMV enhancer/chicken β-actin promoter), a CTLA4-Ig or CD40-Ig transgene-encoding sequence, and a bovine growth hormone (BGH) polyA signal. AAV vector production, purification, and titration were performed as previously described.[37]

Mice

Female C57BL/6J mice (9–12 weeks old) were purchased from the JiSui Biology Company (Nanjing, China). All mice were bred under

Figure 5. The therapeutic effect of AAV therapy on inflammatory cytokines and pathological signs

Cytokines TNF-α, IFN-γ, IL-1β, IL-6, IL-17, and IL-23 from the lumbar spinal cord (A) and spleen (B) were tested through qRT-PCR (n = 5 per group). (C) LFB staining of demyelination is shown (n = 5 per group). The scale bar in the upper row represents 500 μm and in the lower row 100 μm. Red arrows indicate demyelination regions. Statistical analysis is shown in the right panel. Each value represents the mean ± SEM. $^{*}p < 0.05$, $^{**}p < 0.01$, and $^{***}p < 0.001$, compared with control. One-way ANOVA followed by Dunnett posttest is shown.

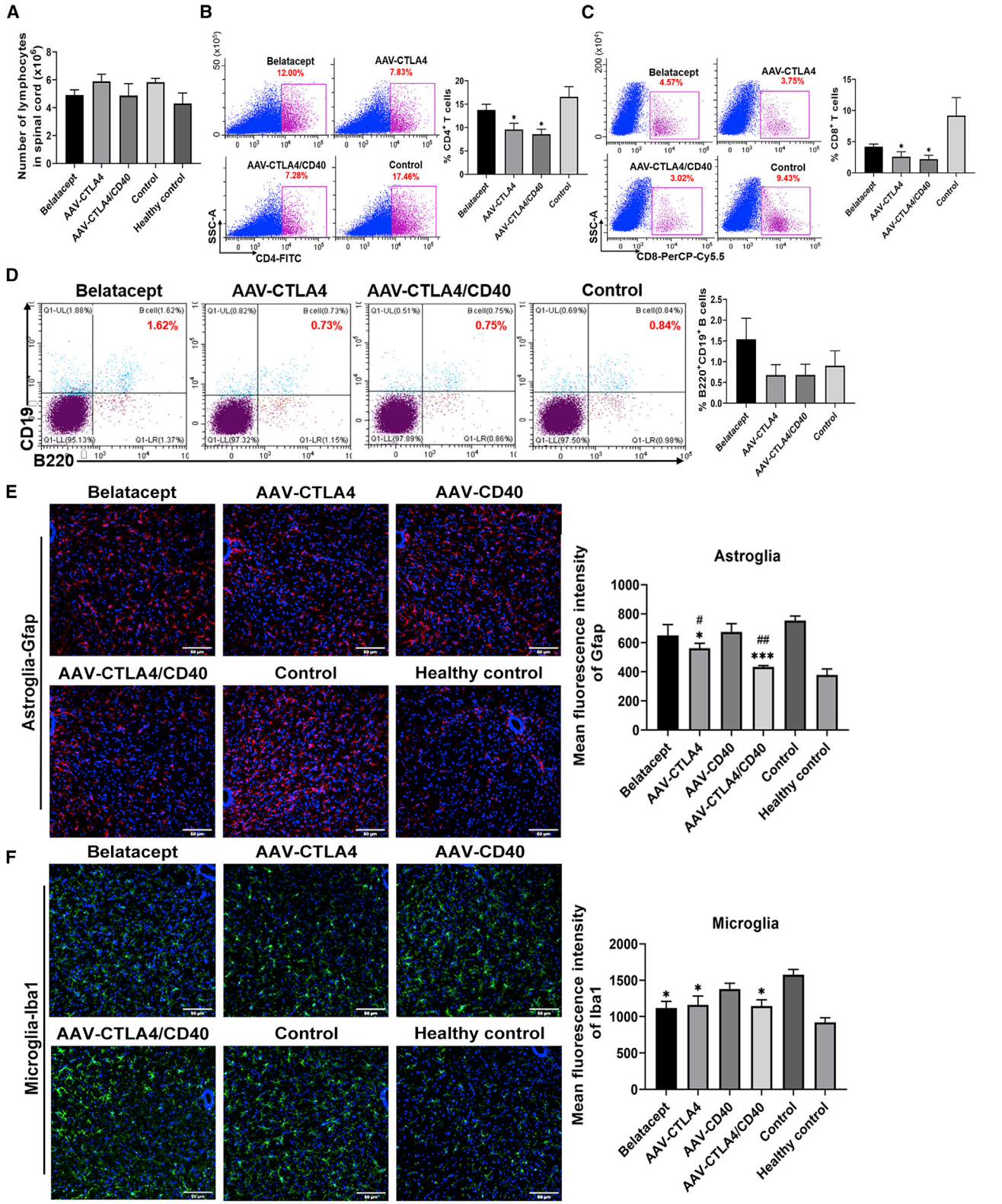

(legend on next page)

standard conditions at the Beautiful Life Medical Technology (Shanghai, China). The animal protocols were approved by the University of North Carolina at Chapel Hill Institutional Animal Care and Use Committee.

EAE induction and AAV administration

EAE was induced in C57BL/6 mice with a subcutaneous injection of MOG_{35-55} in complete Freund's adjuvant (CFA) (Hooke Labs, Lawrence, MA, USA), followed by an intraperitoneal injection of 200 ng pertussis toxin (PTX), first on the day of immunization (day 0) and then on the following day (day 1), according to the recommended protocol. EAE is scored on a scale of 0.0–5.0: 0.0, no obvious changes in motor function; 0.5, limp tip of tail; 1.0, limp tail; 1.5, hind leg inhibition; 2.0, weakness of hind legs; 2.5, dragging of hind legs; 3.0, almost complete paralysis of hind legs; 3.5, complete paralysis of hind legs; 4.0, partial front leg paralysis; 4.5, no movement around the cage; and 5.0, dead due to paralysis.

To determine the prophylactic effect of AAV administration, the mice (n = 8–10 per group) were injected intravenously with AAV8 with a dose of 2×10^{12} vg/kg 14 days before EAE induction. To determine the therapeutic effect of AAV, the mice (n = 8–10 per group) were injected with AAV8 with a dose of 5×10^{12} vg/kg when their MCS was 2.0. Since the MCS for individual mice reached 2.0 at different points in time, AAV injections were administered between 11 and 14 days. To compare AAV treatments with recombinant CTLA4-Ig (belatacept), the mice (n = 8–10 per group) were intravenously injected with AAV8 with a dose of 5×10^{12} vg/kg 4 days after EAE induction. In the belatacept group, mice were administered intraperitoneally 100 μg belatacept (BMS) every alternate day for seven doses, beginning 4 days after EAE induction. The dose of belatacept referred to previous study.[24] The control group consisted of EAE mice not receiving treatment; untreated wild-type mice were used as healthy controls.

ELISA

Human CTLA4-Ig and CD40-Ig expression in the serum were quantified using CTLA4 (Thermo Fisher Scientific) and CD40 ELISA kits (R&D Systems, Minneapolis, MN), respectively. ALT and AST were tested by two types of ELISA kits (Mlbio, Shanghai, China and Ybiotech, Shanghai, China). All procedures were performed according to the manufacturers' instructions.

IgG against MOG assay

Toward the end of the study, serum samples were obtained to determine levels of IgG against MOG according to a previously described method.[55] Ten micrograms per milliliter MOG_{35-55} peptides were coated in a carbonate buffer on 96-well plates at 4°C overnight. The wells were blocked with 1% dry milk in phosphate buffer saline (PBS) with Tween 20 at room temperature (RT) for 1 h. After washing with 0.05% Tween 20 in PBS, diluted serum samples were added and incubated at RT for 2 h. Next, the plates were washed and incubated with horseradish peroxidase (HRP)-conjugated anti-mouse IgG (Abcam) at RT for 1 h. After washing, the 3,3′5,5′-tetramethylbenzidine substrate (Sigma-Aldrich) was added at RT for 10 min. Finally, the reaction was stopped with 1 N sulfuric acid, and optical density (OD) values were measured at 450 nm.

Flow cytometry

Mice were perfused intracardially with cold PBS, and the spinal cord was immediately collected on ice. Lymphocytes were purified using Ficoll Paque Premium 1.084 (GE Healthcare). Total lymphocyte number was measured using Automated Cell counter (Corning, NY, USA). Single-cell suspensions were stained with surface markers anti-CD4 (fluorescein isothiocyanate [FITC]), anti-CD8 (PerCP-Cy5.5), anti-B220 (allophycocyanin [APC]), and anti-CD19 (phycoerythrin [PE]). All antibodies were purchased from BD Biosciences, and the procedures were performed according to the manufacturers' instructions. The samples were analyzed using CytoFLEX flow cytometer (Beckman Coulter, Brea, CA), and data were analyzed using CytExpert 2.0 (Beckman) or FlowJo (v.10.6.2).

Immunofluorescence

Murine spinal cords were collected, fixed in 4% paraformaldehyde, dehydrated in 10%–30% saccharose, and sliced into 20 μm frozen sections. The astroglia and microglia were tested for specific markers of glial fibrillary acidic protein (Gfap) (MAB360, Chemicon) and ionized calcium binding adapter molecule 1 (Iba1) (019-19741, WAKO). The slices were visualized at 20× and 40× magnification under a confocal laser scanning microscope (Nikon, Melville, USA). Integrated fluorescence intensities were determined in three fields per slice and five slices per mouse using the ImageJ software.

Real-time qPCR

To investigate inflammatory cytokines in the spinal cord and spleen, total RNA was extracted from tissues using TRIzol reagent (Thermo Fisher Scientific, Waltham, MA) according to the manufacturers' instructions. RNA was then reverse transcribed to cDNA using Prime Script RT Master Mix (Takara Bio USA), following the procedure recommended by the manufacturer. The cDNA samples were amplified by qPCR using ChamQ SYBR qPCR Master Mix (Vazyme Biotech, Nanjing, China) under Real-Time PCR System qTOWER2.0 (Analytik Jena AG, Germany). The sequence of primers was TNF-α: forward (5′-GATCGGTCCCCAAAGGGATG-3′) and reverse (5′-GTTTGC TACGACGTGGGCTA-3′); IFN-γ: forward (5′-AACGCTACACAC TGCATCT-3′) and reverse (5′-GAGCTCATTGAATGCTTGG-3′); IL-1β: forward (5′-GAAATGCCACCTTTTGACAGTG-3′) and

Figure 7. Comparison of gene therapy and CTLA4-Ig therapy on immune cells

(A) At day 45, total number of lymphocytes from spinal cord were measured. The percentages of $CD4^+$ T (B), $CD8^+$ T (C), and $B220^+CD19^+$ B cells (D) were examined by flow cytometry (n = 4–6 per group). Amounts of astroglia (E) and microglia (F) in the spinal cord were assayed with specific markers Gfap and Iba1 by immunofluorescence (n = 5 per group). Representative images of integrated fluorescence intensity were quantified. The scale bar represents 50 μm. Each value represents the mean ± SEM. $^*p < 0.05$ and $^{***}p < 0.001$, compared with control; $^{\#}p < 0.05$ and $^{\#\#}p < 0.01$, compared with belatacept. One-way ANOVA followed by Tukey posttest is shown.

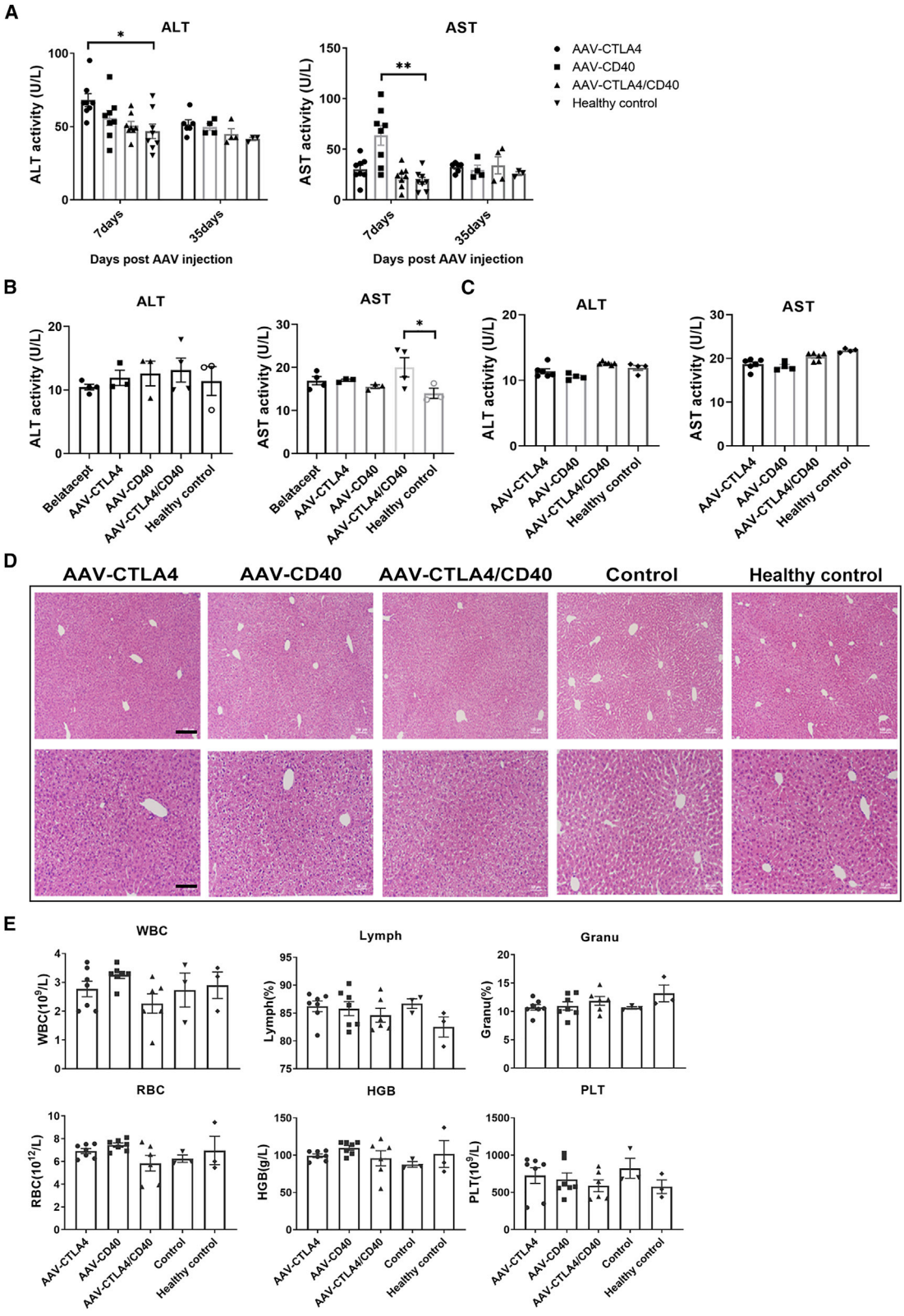

(legend on next page)

reverse (5′-TGGATGCTCTCATCAGGACAG-3′); IL-6: forward (5′-CACTTCACAAGTCGGAGGCTT-3′) and reverse (5′-TCAGAATTGCCATTGCACAAC-3′); IL-17: forward (5′-GCTCCAGAAGGCCCTCAGA-3′) and reverse (5′-AGCTTTCCCTCCGCATTGA-3′); IL-23: forward (5′-AGTGCCAGCAGCTCTCTCGGA-3′) and reverse (5′-GCCAGACCTTGGCGGATCCTTT-3′); and GAPDH: forward (5′-AAGGTCATCCCAGAGCTGAA-3′) and reverse (5′-CTGCTTCACCACCTTCTTGA-3′) as quantified reference gene primers. Relative expression was calculated according to the $2^{-\Delta\Delta CT}$ method,[61] and expression per sample was conducted in quadruplicate. Results were expressed relative to the mean of the control mice, which was set at 1.

Histopathology

Mice spinal cord were collected, fixed in 4% paraformaldehyde, dehydrated in 10%–30% saccharose, and sliced into 5-μm paraffin sections. To investigate inflammation and demyelination of the white matter, slices were stained with H&E and LFB. Immunohistochemistry of CD4 and CD8 antibodies followed standard procedures by the manufacturer. The slices were visualized at 4×, 20×, or 10× magnification under an orthographic microscope (Nikon, Melville, USA). Histological analyses were performed in four fields per slice and five slices per mouse. Inflammation foci and demyelination were observed using serial cut sections from the same mouse. White matter of the spinal cord was selected for analysis with the ImageJ software. The bar graphs show the percentage of inflammation, demyelination, or CD4- or CD8-positive area in the total white matter.

Hematologic analysis

The mouse blood was collected from the orbit in tubes with K_2EDTA anticoagulant (BD Biosciences). Peripheral blood cells, including white blood cells, lymphocytes, granulocytes, red blood cells, hemoglobin, and platelets, were tested using the Automatic Animal Hematology Analyzer (BC-2800vet, Shenzhen, China) following the manufacturer's instructions.

Statistical analysis

Statistical analyses were performed using GraphPad Prism (v.8.0.2). Data were shown as mean ± SEM. One-way or two-way ANOVA was used for multiple testing. *$p < 0.05$, **$p < 0.01$, or ***$p < 0.001$ was considered statistically significant.

ACKNOWLEDGMENTS

This work was supported by the Fundamental Research Funds for the Central Universities (grant number 81970171).

AUTHOR CONTRIBUTIONS

C.Z., C.C., X.W., and X.X. designed the experiments; C.Z., Z.C., and Y.X. performed experiments; C.Z. analyzed data and wrote the manuscript; C.Z., C.C., and X.W. revised the manuscript; and J.W. and F.Z. contributed helpful advice.

DECLARATION OF INTERESTS

The authors declare no competing interests.

REFERENCES

1. Dobson, R., and Giovannoni, G. (2019). Multiple sclerosis - a review. Eur. J. Neurol. *26*, 27–40. https://doi.org/10.1111/ene.13819.

2. Ascherio, A. (2013). Environmental factors in multiple sclerosis. Expert Rev. Neurother. *13*, 3–9. https://doi.org/10.1586/14737175.2013.865866.

3. Reynolds, E.R., Ashbaugh, A.D., Hockenberry, B.J., and McGrew, C.A. (2018). Multiple sclerosis and exercise: a literature review. Curr. Sports Med. Rep. *17*, 31–35. https://doi.org/10.1249/JSR.0000000000000446.

4. Comi, G. (2013). Disease-modifying treatments for progressive multiple sclerosis. Mult. Scler. *19*, 1428–1436. https://doi.org/10.1177/1352458513502572.

5. Correale, J., Gaitán, M.I., Ysrraelit, M.C., and Fiol, M.P. (2017). Progressive multiple sclerosis: from pathogenic mechanisms to treatment. Brain *140*, 527–546. https://doi.org/10.1093/brain/aww258.

6. Giovannoni, G., Radue, E.W., Havrdova, E., Riester, K., Greenberg, S., Mehta, L., and Elkins, J. (2014). Effect of daclizumab high-yield process in patients with highly active relapsing-remitting multiple sclerosis. J. Neurol. *261*, 316–323. https://doi.org/10.1007/s00415-013-7196-4.

7. Gross, C.C., Schulte-Mecklenbeck, A., Runzi, A., Kuhlmann, T., Posevitz-Fejfár, A., Schwab, N., Schneider-Hohendorf, T., Herich, S., Held, K., Konjevic, M., et al. (2016). Impaired NK-mediated regulation of T-cell activity in multiple sclerosis is reconstituted by IL-2 receptor modulation. Proc. Natl. Acad. Sci. USA *113*, E2973–E2982. https://doi.org/10.1073/pnas.1524924113.

8. Kappos, L., Bar-Or, A., Cree, B., Fox, R., Giovannoni, G., Gold, R., Vermersch, P., Arnould, S., Sidorenko, T., Wolf, C., et al. (2016). Efficacy and safety of siponimod in secondary progressive multiple sclerosis-results of the placebo controlled, double-blind, Phase III EXPAND study. In Proceedings of the 32nd Congress of the European Committee for Treatment and Research in Multiple Sclerosis (ECTRIMS).

9. Cohen, J.A., Cutter, G.R., Fischer, J.S., Goodman, A.D., Heidenreich, F.R., Kooijmans, M.F., Sandrock, A.W., Rudick, R.A., Simon, J.H., Simonian, N.A., et al. (2002). Benefit of interferon beta-1a on MSFC progression in secondary progressive MS. Neurology *59*, 679–687. https://doi.org/10.1212/wnl.59.5.679.

10. Andersen, O., Elovaara, I., Färkkilä, M., Hansen, H.J., Mellgren, S.I., Myhr, K.M., Sandberg-Wollheim, M., and Soelberg, Sørensen, P. (2004). Multicentre, randomised, double blind, placebo controlled, phase III study of weekly, low dose, subcutaneous interferon beta-1a in secondary progressive multiple sclerosis. J. Neurol. Neurosurg. Psychiatry *75*, 706–710. https://doi.org/10.1136/jnnp.2003.010090.

11. Panitch, H., Miller, A., Paty, D., and Weinshenker, B. (2004). Interferon beta-1b in secondary progressive MS: results from a 3-year controlled study. Neurology *63*, 1788–1795. https://doi.org/10.1212/01.wnl.0000146958.77317.3e.

12. Reich, D.S., Lucchinetti, C.F., and Calabresi, P.A. (2018). Multiple sclerosis. N. Engl. J. Med. *378*, 169–180. https://doi.org/10.1056/nejmra1401483.

13. Mcfarland, H.F., and Martin, R. (2007). Multiple sclerosis: a complicated picture of autoimmunity. Nat. Immunol. *8*, 913–919. https://doi.org/10.1038/ni1507.

Figure 8. Safety evaluation of long-term expression of immune-inhibitory proteins delivered by AAV

(A) Chronic hepatotoxicity including plasma ALT and AST levels was assayed at 7 and 35 days post-injection in the prophylactic experiment. Plasma ALT and AST levels in mice receiving AAV at early (B) and end-stage EAE (C) were tested at the end of therapeutic experiments. *$p < 0.05$ and **$p < 0.01$, compared with healthy control. One-way ANOVA followed by Dunnett posttest is shown. (D) H&E staining of liver tissues of mice receiving AAV at end-stage EAE was assayed. The scale bar in the upper row represents 200 μm and in the lower row 100 μm. (E) Hematotoxicity was performed and included white blood cells (WBC), lymphocytes (Lymph), granulocytes (Granu), red blood cells (RBC), hemoglobin (HGB), and platelets (PLT) from peripheral blood (n = 3–8 per group). One-way ANOVA followed by Tukey posttest is shown. Each value represents the mean ± SEM.

14. Durelli, L., Conti, L., Clerico, M., Boselli, D., Contessa, G., Ripellino, P., Ferrero, B., Eid, P., and Novelli, F. (2009). T-helper 17 cells expand in multiple sclerosis and are inhibited by interferon-β. Ann. Neurol. *65*, 499–509. https://doi.org/10.1002/ana.21652.

15. Baecher-Allan, C., Kaskow, B.J., and Weiner, H.L. (2018). Multiple sclerosis: mechanisms and immunotherapy. Neuron *97*, 742–768. https://doi.org/10.1016/j.neuron.2018.01.021.

16. Tzartos, J.S., Friese, M.A., Craner, M.J., Palace, J., Newcombe, J., Esiri, M.M., and Fugger, L. (2008). Interleukin-17 production in central nervous system-infiltrating T cells and glial cells is associated with active disease in multiple sclerosis. Am. J. Pathol. *172*, 146–155. https://doi.org/10.2353/ajpath.2008.070690.

17. Lock, C., Hermans, G., Pedotti, R., Brendolan, A., Schadt, E., Garren, H., Langer-Gould, A., Strober, S., Cannella, B., Allard, J., et al. (2002). Gene-microarray analysis of multiple sclerosis lesions yields new targets validated in autoimmune encephalomyelitis. Nat. Med. *8*, 500–508. https://doi.org/10.1038/nm0502-500.

18. Traugott, U., Reinherz, E.L., and Raine, C.S. (1983). Multiple sclerosis. Distribution of T cells, T cell subsets and Ia-positive macrophages in lesions of different ages. J. Neuroimmunol. *4*, 201–221. https://doi.org/10.1016/0165-5728(83)90036-x.

19. Hauser, S.L., Aubert, C., Burks, J.S., Kerr, C., Lyon-Caen, O., de The, G., and Brahic, M. (1986). Analysis of human T-lymphotropic virus sequences in multiple sclerosis tissue. Nature *322*, 176–177. https://doi.org/10.1038/322176a0.

20. Hauser, S.L., Waubant, E., Arnold, D.L., Vollmer, T., Antel, J., Fox, R.J., Bar-Or, A., Panzara, M., Sarkar, N., Agarwal, S., et al. (2008). B-cell depletion with rituximab in relapsing-remitting multiple sclerosis. N. Engl. J. Med. *358*, 676–688. https://doi.org/10.1056/nejmoa0706383.

21. Greenfield, A.L., and Hauser, S.L. (2018). B-cell therapy for multiple sclerosis: entering an era. Ann. Neurol. *83*, 13–26. https://doi.org/10.1002/ana.25119.

22. van Langelaar, J., Rijvers, L., Smolders, J., and van Luijn, M.M. (2020). B and T Cells driving multiple sclerosis: identity, mechanisms and potential triggers. Front. Immunol. *11*, 760. https://doi.org/10.3389/fimmu.2020.00760.

23. Perrin, P.J., Scott, D., Quigley, L., Albert, P.S., Feder, O., Gray, G.S., Abe, R., June, C.H., and Racke, M.K. (1995). Role of B7:CD28/CTLA-4 in the induction of chronic relapsing experimental allergic encephalomyelitis. J. Immunol. *154*, 1481–1490.

24. Vanderlugt, C.L., Begolka, W.S., Neville, K.L., Katz-Levy, Y., Howard, L.M., and Eagar, T.N. (1998). The functional significance of epitope spreading and its regulation by co-stimulatory molecules. Immunol. Rev. *164*, 63–72. https://doi.org/10.1111/j.1600-065x.1998.tb01208.x.

25. Howard, L.M., Miga, A.J., Vanderlugt, C.L., Canto, M.C.D., Laman, J.D., Noelle, R.J., and Miller, S.D. (1999). Mechanisms of immunotherapeutic intervention by anti-CD40L (CD154) antibody in an animal model of multiple sclerosis. J. Clin. Invest. *103*, 281–290. https://doi.org/10.1172/jci5388.

26. Finck, B.K., Linsley, P.S., and Wofsy, D. (1994). Treatment of murine lupus with CTLA4Ig. Science *265*, 1225–1227. https://doi.org/10.1126/science.7520604.

27. Mohan, C., Shi, Y., Laman, J.D., and Datta, S.K. (1995). Interaction between CD40 and its ligand gp39 in the development of murine lupus nephritis. J. Immunol. *154*, 1470–1480.

28. Schaub, M., Issazadeh, S., Stadlbauer, T.H., Peach, R., Sayegh, M.H., and Khoury, S.J. (1999). Costimulatory signal blockade in murine relapsing experimental autoimmune encephalomyelitis. J. Neuroimmunol. *96*, 158–166. https://doi.org/10.1016/s0165-5728(99)00022-3.

29. Khoury, S.J., Rochon, J., Ding, L., Byron, M., Ryker, K., Tosta, P., Gao, W., Freedman, M.S., Arnold, D.L., Sayre, P.H., and Smilek, D.E.; On behalf of the ACCLAIM Study Group (2017). ACCLAIM: a randomized trial of abatacept (CTLA4-Ig) for relapsing-remitting multiple sclerosis. Mult. Scler. *23*, 686–695. https://doi.org/10.1177/1352458516662727.

30. Glatigny, S., Höllbacher, B., Motley, S.J., Tan, C., Hundhausen, C., Buckner, J.H., Smilek, D., Khoury, S.J., Ding, L., Qin, T., et al. (2019). Abatacept targets T follicular helper and regulatory T Cells, disrupting molecular pathways that regulate their proliferation and maintenance. J. Immunol. *202*, 1373–1382. https://doi.org/10.4049/jimmunol.1801425.

31. Athanasopoulos, T., Graham, I.R., Foster, H., and Dickson, G. (2004). Recombinant adeno-associated viral (rAAV) vectors as therapeutic tools for Duchenne muscular dystrophy (DMD). Gene Ther. *11*, S109–S121. https://doi.org/10.1038/sj.gt.3302379.

32. Ram, S.E., and Galun, E. (2009). AAV2-GDNF gene therapy for Parkinson's disease. Hum. Gene Ther. *20*, 430–431. https://doi.org/10.1089/hum.2009.1599.

33. Sun, L., Qi, X., Hauswirth, W.W., and Guy, J. (2003). AAV-mediated sod2 gene expression driven by a pro-inflammatory inducible promoter: a novel method for gene therapy of multiple sclerosis. Arvo. Meet. Abstr. *44*.

34. Miralles, M., Eixarch, H., Tejero, M., Costa, C., Hirota, K., Castaño, A.R., Puig, M., Stockinger, G., Montalban, X., Bosch, A., et al. (2017). Clinical and histopathological amelioration of experimental autoimmune encephalomyelitis by AAV Vectors expressing a soluble interleukin-23 receptor. Neurotherapeutics *14*, 1095–1106. https://doi.org/10.1007/s13311-017-0545-8.

35. Keeler, G.D., Kumar, S., Palaschak, B., Silverberg, E.L., Markusic, D.M., Jones, N.T., and Hoffman, B.E. (2018). Gene therapy-induced antigen-specific Tregs inhibit neuro-inflammation and reverse disease in a mouse model of multiple sclerosis. Mol. Ther. *26*, 173–183. https://doi.org/10.1016/j.ymthe.2017.09.001.

36. Vasquez, M., Consuegra-Fernández, M., Aranda, F., Jimenez, A., Tenesaca, S., Fernandez-Sendin, M., Gomar, C., Ardaiz, N., Di Trani, C.A., Casares, N., et al. (2019). Treatment of experimental autoimmune encephalomyelitis by sustained delivery of low-dose IFN-α. J. Immunol. *203*, 696–704. https://doi.org/10.4049/jimmunol.1801462.

37. Ye, X., Zhu, T., Bastacky, S., McHale, T., Li, J., and Xiao, X. (2005). Prevention and reversal of lupus in NZB/NZW mice by costimulatory blockade with adeno-associated virus-mediated gene transfer. Arthritis Rheum. *52*, 3975–3986. https://doi.org/10.1002/art.21417.

38. Ponomarev, E.D., Shriver, L.P., Maresz, K., and Dittel, B.N. (2005). Microglial cell activation and proliferation precedes the onset of CNS autoimmunity. J. Neurosci. Res. *81*, 374–389. https://doi.org/10.1002/jnr.20488.

39. Goverman, J. (2009). Autoimmune T cell responses in the central nervous system. Nat. Rev. Immunol. *9*, 393–407. https://doi.org/10.1038/nri2550.

40. Cross, A.H., Girard, T.J., Giacoletto, K.S., Evans, R.J., Keeling, R.M., Lin, R.F., Trotter, J.L., and Karr, R.W. (1995). Long-term inhibition of murine experimental autoimmune encephalomyelitis using CTLA-4-Fc supports a key role for CD28 costimulation. J. Clin. Invest. *95*, 2783–2789. https://doi.org/10.1172/jci117982.

41. Khoury, S.J., Akalin, E., Chandraker, A., Turka, L.A., Linsley, P.S., Sayegh, M.H., and Hancock, W.W. (1995). CD28-B7 costimulatory blockade by CTLA4Ig prevents actively induced experimental autoimmune encephalomyelitis and inhibits Th1 but spares Th2 cytokines in the central nervous system. J. Immunol. *155*, 4521–4524.

42. Kuchroo, V.K., Prabhu Das, M., Brown, J.A., Ranger, A.M., Zamvil, S.S., Sobel, R.A., Weiner, H.L., Nabavi, N., and Glimcher, L.H. (1995). B7-1 and B7-2 costimulatory molecules activate differentially the Th1/Th2 developmental pathways: application to autoimmune disease therapy. Cell *80*, 707–718. https://doi.org/10.1016/0092-8674(95)90349-6.

43. Miller, S.D., Vanderlugt, C.L., Lenschow, D.J., Pope, J.G., Karandikar, N.J., Dal Canto, M.C., and Bluestone, J.A. (1995). Blockade of CD28/B7-1 interaction prevents epitope spreading and clinical relapses of murine EAE. Immunity *3*, 739–745. https://doi.org/10.1016/1074-7613(95)90063-2.

44. Perrin, P.J., Scott, D., Davis, T.A., Gray, G.S., Doggett, M.J., Abe, R., June, C.H., and Racke, M.K. (1996). Opposing effects of CTLA4-Ig and anti-CD80 (B7-1) plus anti-CD86 (B7-2) on experimental allergic encephalomyelitis. J. Neuroimmunol. *65*, 31–39. https://doi.org/10.1016/0165-5728(95)00172-7.

45. Gerritse, K., Laman, J.D., Noelle, R.J., Aruffo, A., Ledbetter, J.A., Boersma, W.J., and Claassen, E. (1996). CD40-CD40 ligand interactions in experimental allergic encephalomyelitis and multiple sclerosis. Proc. Natl. Acad. Sci. USA *93*, 2499–2504. https://doi.org/10.1073/pnas.93.6.2499.

46. Maheshri, N., Koerber, J.T., Kaspar, B.K., and Schaffer, D.V. (2006). Directed evolution of adeno-associated virus yields enhanced gene delivery vectors. Nat. Biotechnol. *24*, 198–204. https://doi.org/10.1038/nbt1182.

47. Zhong, C., Jiang, W., Wang, Y., Sun, J., Wu, X., Zhuang, Y., and Xiao, X. (2021). Repeated systemic dosing of AAV vectors in immunocompetent mice after blockade of T-cell costimulatory pathways. Hum. Gene. Ther. *33*. Epub ahead of print. https://doi.org/10.1089/hum.2021.129.

48. Grewal, I.S., Foellmer, H.G., Grewal, K.D., Xu, J., Hardardottir, F., Baron, J.L., Janeway, C.A., Jr., and Flavell, R.A. (1996). Requirement for CD40 ligand in

costimulation induction, T cell activation, and experimental allergic encephalomyelitis. Science *273*, 1864–1867. https://doi.org/10.1126/science.273.5283.1864.

49. Aarts, S.A.B.M., Seijkens, T.T.P., van Dorst, K.J.F., Dijkstra, C.D., Kooij, G., and Lutgens, E. (2017). The CD40-CD40L dyad in experimental autoimmune encephalomyelitis and multiple sclerosis. Front. Immunol. *8*, 1791. https://doi.org/10.3389/fimmu.2017.01791.

50. Antel, J., and Bar-Or, A. (2006). Roles of immunoglobulins and B cells in multiple sclerosis: from pathogenesis to treatment. J. Neuroimmunol. *180*, 3–8. https://doi.org/10.1016/j.jneuroim.2006.06.032.

51. Fillatreau, S., Gray, D., and Anderton, S.M. (2008). Not always the bad guys: B cells as regulators of autoimmune pathology. Nat. Rev. Immunol. *8*, 391–397. https://doi.org/10.1038/nri2315.

52. Ramgolam, V.S., Sha, Y., Marcus, K.L., Choudhary, N., Troiani, L., Chopra, M., and Markovic-Plese, S. (2011). B cells as a therapeutic target for IFN-β in relapsing-remitting multiple sclerosis. J. Immunol. *186*, 4518–4526. https://doi.org/10.4049/jimmunol.1000271.

53. Xiao, B.G., Linington, C., and Link, H. (1991). Antibodies to myelin-oligodendrocyte glycoprotein in cerebrospinal fluid from patients with multiple sclerosis and controls. J. Neuroimmunol. *31*, 91–96. https://doi.org/10.1016/0165-5728(91)90014-x.

54. Sun, J., Link, H., Olsson, T., Xiao, B.G., Andersson, G., Ekre, H.P., Linington, C., and Diener, P. (1991). T and B cell responses to myelin-oligodendrocyte glycoprotein in multiple sclerosis. J. Immunol. *146*, 1490–1495.

55. Komiyama, Y., Nakae, S., Matsuki, T., Nambu, A., Ishigame, H., Kakuta, S., Sudo, K., and Iwakura, Y. (2006). IL-17 plays an important role in the development of experimental autoimmune encephalomyelitis. J. Immunol. *177*, 566–573. https://doi.org/10.4049/jimmunol.177.1.566.

56. Kohm, A.P., Carpentier, P.A., Anger, H.A., and Miller, S.D. (2002). $CD4^+CD25^+$ regulatory T cells suppress antigen-specific autoreactive immune responses and central nervous system inflammation during active experimental autoimmune encephalomyelitis. J. Immunol. *169*, 4712–4716. https://doi.org/10.4049/jimmunol.169.9.4712.

57. Liddelow, S.A., Guttenplan, K.A., Clarke, L.E., Bennett, F.C., Bohlen, C.J., Schirmer, L., Bennett, M.L., Munch, A.E., Chung, W.S., Peterson, T.C., et al. (2017). Neurotoxic reactive astrocytes are induced by activated microglia. Nature *541*, 481–487. https://doi.org/10.1038/nature21029.

58. Correale, J., and Farez, M.F. (2015). The role of astrocytes in multiple sclerosis progression. Front. Neurol. *6*, 180. https://doi.org/10.3389/fneur.2015.00180.

59. Lassmann, H. (2014). Multiple sclerosis: lessons from molecular neuropathology. Exp. Neurol. *262*, 2–7. https://doi.org/10.1016/j.expneurol.2013.12.003.

60. Srinivas, N.R., Weiner, R.S., Shyu, W.C., Calore, J.D., Tritschler, D., Tay, L.K., Lee, J.S., Greene, D.S., and Barbhaiya, R.H. (1996). A pharmacokinetic study of intravenous CTLA4Ig, a novel immunosuppressive agent, in mice. J. Pharm. Sci. *85*, 296–298. https://doi.org/10.1021/js950428+.

61. Kenneth, J.L., and Thomas, D.S. (2002). Analysis of relative gene expression data using real-time quantitative PCR and the $2^{-\Delta\Delta Ct}$ method. Methods *25*, 402–408.